

DESY 06-092
 MS-TP-06-2
 BNL-HET-06/3

Numerical simulation of QCD with u , d , s and c quarks in the twisted-mass Wilson formulation

T. Chiarappa^a, F. Farchioni^b, K. Jansen^c, I. Montvay^d,
 E.E. Scholz^e, L. Scorzato^f, T. Sudmann^b, C. Urbach^g

^a Università Milano Bicocca, Piazza della Scienza 3, I-20126 Milano, Italy

^b Universität Münster, Institut für Theoretische Physik,
 Wilhelm-Klemm-Strasse 9, D-48149 Münster, Germany

^c NIC, DESY, Zeuthen, Platanenallee 6, D-15738 Zeuthen, Germany

^d Deutsches Elektronen-Synchrotron DESY, Notkestr. 85, D-22603 Hamburg, Germany

^e Physics Department, Brookhaven National Laboratory, Upton, NY 11973 USA

^f ECT* strada delle tabarelle 286, 38050 Villazzano (TN), Italy

^g Theoretical Physics Division, Dept. of Mathematical Sciences,
 University of Liverpool, Liverpool L69 3BX, UK

Abstract

A first study of numerical Monte Carlo simulations with two quark doublets, a mass-degenerate one and a mass-split one, interpreted as u , d , s and c quarks, is carried out in the framework of the twisted mass Wilson lattice formulation. Tuning the bare parameters of this theory is explored on $12^3 \cdot 24$ and $16^3 \cdot 32$ lattices at lattice spacings $a \simeq 0.20$ fm and $a \simeq 0.15$ fm, respectively.

1 Introduction

In QCD the effect of virtual quark loops is most important for the three light quarks (u, d, s). In recent unquenched numerical simulations, besides the two lightest quarks u and d , the s -quark is also included (see, for instance, [1, 2]). The formulation of QCD with twisted-mass Wilson fermions [3] is based on chiral rotations of the bare mass (or, equivalently, of the Wilson-term) within quark doublets. Therefore, in this formulation there are two possibilities for unquenched simulations with (u, d, s) quarks: either the s quark is taken alone and the twisted mass formulation is restricted to the (u, d) doublet or, in addition to the s quark, also the c -quark is included in a mass-split doublet using the formulation in Ref. [4]. In the present paper we explore the latter possibility (for first results along this line see the proceedings contribution [5]).

Numerical simulations with twisted-mass Wilson fermions are usually performed at (or near) the critical (untwisted) bare quark mass, because there an *automatic $\mathcal{O}(a)$ improvement of the continuum limit* is expected [6]. Our collaboration has performed several studies of twisted-mass QCD both in the quenched approximation [7], [8], [9], [10] and in unquenched simulations with dynamical (u, d) quarks [11], [12], [13], [14]. In the present paper we explore the possibility of numerical simulations of QCD with a degenerate doublet (u, d) and an mass-split doublet (c, s) of dynamical quarks in the twisted mass Wilson formulation.

The plan of this paper is as follows: in the next section we define the lattice action and describe the simulation algorithm. Section 3 is devoted to the introduction of physical fields and currents important for the interpretation of results. In Section 4 we present our numerical results. The last section contains a discussion and final remarks.

2 Lattice action and simulation algorithm

2.1 Lattice action

The notation for the lattice action of the *light* mass-degenerate (u, d)-doublet, denoted by a subscript l , is the same as in our previous papers, for instance, Ref. [14]:

$$\begin{aligned}
 S_l &= \sum_x \left\{ \left(\bar{\chi}_{l,x} [\mu_{\kappa l} + i\gamma_5 \tau_3 a\mu_l] \chi_{l,x} \right) - \frac{1}{2} \sum_{\mu=\pm 1}^{\pm 4} \left(\bar{\chi}_{l,x+\hat{\mu}} U_{x\mu} [r + \gamma_\mu] \chi_{l,x} \right) \right\} \\
 &\equiv \sum_{x,y} \bar{\chi}_{l,x} Q_{l,xy}^{(\chi)} \chi_{l,y} .
 \end{aligned} \tag{1}$$

Here, and in most cases below, colour-, spinor- and isospin indices are suppressed. For the isospin indices later on we shall also use notations as, for instance, $\chi_l \equiv (\chi_u \ \chi_d)$.

The (“untwisted”) bare quark mass of the light doublet in lattice units is denoted by

$$\mu_{\kappa l} \equiv am_{0l} + 4r = \frac{1}{2\kappa_l} , \quad (2)$$

r is the Wilson-parameter, set in our simulations to $r = 1$, am_{0l} is another convention for the bare quark mass in lattice units and κ_l is the conventional hopping parameter. The twisted mass of the light doublet in lattice units is denoted by $a\mu_l$. $U_{x\mu} \in \text{SU}(3)$ is the gauge link variable and we also defined $U_{x,-\mu} = U_{x-\hat{\mu},\mu}^\dagger$ and $\gamma_{-\mu} = -\gamma_\mu$.

Besides the quark doublet fields $\chi_l, \bar{\chi}_l$ in (1) it will turn out convenient to introduce other fields by the transformation

$$\psi_{l,x} \equiv \frac{1}{\sqrt{2}} (1 + i\gamma_5 \tau_3) \chi_{l,x} , \quad \bar{\psi}_{l,x} \equiv \bar{\chi}_{l,x} \frac{1}{\sqrt{2}} (1 + i\gamma_5 \tau_3) . \quad (3)$$

The *quark matrix on the χ -basis* $Q_l^{(\chi)}$ defined in (1) is

$$Q_{l,xy}^{(\chi)} = \delta_{xy} (\mu_{\kappa l} + i\gamma_5 \tau_3 a\mu_l) - \frac{1}{2} \sum_{\mu=\pm 1}^{\pm 4} \delta_{x,y+\hat{\mu}} U_{y\mu} [r + \gamma_\mu] \quad (4)$$

or in a short notation, without the site indices,

$$Q_l^{(\chi)} = \mu_{\kappa l} + i\gamma_5 \tau_3 a\mu_l + N + R , \quad (5)$$

with

$$N_{xy} \equiv -\frac{1}{2} \sum_{\mu=\pm 1}^{\pm 4} \delta_{x,y+\hat{\mu}} U_{y\mu} \gamma_\mu , \quad R_{xy} \equiv -\frac{r}{2} \sum_{\mu=\pm 1}^{\pm 4} \delta_{x,y+\hat{\mu}} U_{y\mu} . \quad (6)$$

On the ψ -basis defined in (3) we have the quark matrix

$$Q_l^{(\psi)} = \frac{1}{2} (1 - i\gamma_5 \tau_3) Q_l^{(\chi)} (1 - i\gamma_5 \tau_3) = a\mu_l + N - i\gamma_5 \tau_3 (\mu_{\kappa l} + R) . \quad (7)$$

As it has been shown by Frezzotti and Rossi in Ref. [4], a *real quark determinant* with a mass-split doublet can be obtained if the mass splitting is taken to be orthogonal in isospin space to the twist direction. One could take, for instance, the mass splitting in the τ_1 direction if the twist is in the τ_3 direction, as in (1). It is, however, more natural to exchange the two directions because then the bare mass is diagonal in isospin. In this case, the lattice action of the *heavy* mass-split (c, s) -doublet, denoted by a subscript h , is defined as

$$S_h = \sum_{x,y} \bar{\chi}_{h,x} Q_{h,xy}^{(\chi)} \chi_{h,y} \quad (8)$$

with

$$Q_h^{(\chi)} = \mu_{\kappa h} + i\gamma_5 \tau_1 a\mu_\sigma + \tau_3 a\mu_\delta + N + R . \quad (9)$$

For the isospin indices later on we shall also use notations as, for instance, $\chi_h \equiv (\chi_c \chi_s)$. The ψ -basis is introduced similarly to (3) by

$$\psi_{h,x} \equiv \frac{1}{\sqrt{2}} (1 + i\gamma_5 \tau_1) \chi_{h,x} , \quad \bar{\psi}_{h,x} \equiv \bar{\chi}_{h,x} \frac{1}{\sqrt{2}} (1 + i\gamma_5 \tau_1) \quad (10)$$

and the *quark matrix on the ψ -basis* is for the heavy mass-split doublet

$$Q_h^{(\psi)} = \frac{1}{2} (1 - i\gamma_5 \tau_1) Q_h^{(\chi)} (1 - i\gamma_5 \tau_1) = a\mu_\sigma + \tau_3 a\mu_\delta + N - i\gamma_5 \tau_1 (\mu_{\kappa h} + R) . \quad (11)$$

For the SU(3) Yang-Mills gauge field we apply the *tree-level improved Symanzik* (tlSym) action which belongs to a one-parameter family of actions obtained by renormalisation group considerations and in the Symanzik improvement scheme [15]. Those actions also include, besides the usual (1×1) Wilson loop plaquette term, planar rectangular (1×2) Wilson loops:

$$S_g = \beta \sum_x \left(c_0 \sum_{\mu < \nu; \mu, \nu=1}^4 \left\{ 1 - \frac{1}{3} \text{Re} U_{x\mu\nu}^{1 \times 1} \right\} + c_1 \sum_{\mu \neq \nu; \mu, \nu=1}^4 \left\{ 1 - \frac{1}{3} \text{Re} U_{x\mu\nu}^{1 \times 2} \right\} \right) , \quad (12)$$

with the condition $c_0 = 1 - 8c_1$. For the tlSym action we have $c_1 = -1/12$ [16].

2.2 Simulation algorithm

For preparing the sequences of gauge configurations a *Polynomial Hybrid Monte Carlo* (PHMC) updating algorithm was used. This algorithm is based on multi-step (actually two-step) polynomial approximations of the inverse fermion matrix with stochastic correction in the update chain as described in Ref. [17]. It is based on the PHMC algorithm as introduced in Ref. [18]. The polynomial approximation scheme and the stochastic correction in the update chain is taken over from the two-step multi-boson algorithm of Ref. [19]. (For an alternative updating algorithm in QCD with $N_f = 2 + 1 + 1$ quark flavours, which will be used for algorithmic comparisons in the future, see [20].)

For typical values of the approximation interval and polynomial orders on $16^3 \cdot 32$ lattices see Table 1. The notations are those of Ref. [17]: the approximation interval is $[\epsilon, \lambda]$, the orders of the polynomials P_j ($j = 1, 2$) are n_j and those of \bar{P}_j ($j = 1, 2$) are \bar{n}_j , respectively. The simulations have been done with *determinant break-up* $n_B = 2$. On the $12^3 \cdot 24$, for similar values of the pseudoscalar masses in lattice units, the orders n_2 and \bar{n}_2 are the same and the values of n_1 and \bar{n}_1 are somewhat smaller.

3 Physical fields and currents

The *physical quark fields*, which in the continuum limit are proportional to the renormalised quark fields of both flavours in the doublets, are obtained [3] by a chiral

rotation from the fields in the lattice action in (1) or from those defined in (3) for the light doublet, and similarly in (8)-(10) for the heavy doublet. On the χ -basis we have

$$\psi_{l,x}^{phys} = e^{\frac{i}{2}\omega_l\gamma_5\tau_3}\chi_{l,x}, \quad \bar{\psi}_{l,x}^{phys} = \bar{\chi}_{l,x}e^{\frac{i}{2}\omega_l\gamma_5\tau_3}; \quad (13)$$

$$\psi_{h,x}^{phys} = e^{\frac{i}{2}\omega_h\gamma_5\tau_1}\chi_{h,x}, \quad \bar{\psi}_{h,x}^{phys} = \bar{\chi}_{h,x}e^{\frac{i}{2}\omega_h\gamma_5\tau_1}. \quad (14)$$

Since the transformations in (3) and (10) correspond to chiral rotations with $\omega_l = \frac{\pi}{2}$ and $\omega_h = \frac{\pi}{2}$, respectively, we have with

$$\bar{\omega}_l \equiv \omega_l - \frac{\pi}{2}, \quad \bar{\omega}_h \equiv \omega_h - \frac{\pi}{2} \quad (15)$$

the relations

$$\psi_{l,x}^{phys} = e^{\frac{i}{2}\bar{\omega}_l\gamma_5\tau_3}\psi_{l,x}, \quad \bar{\psi}_{l,x}^{phys} = \bar{\psi}_{l,x}e^{\frac{i}{2}\bar{\omega}_l\gamma_5\tau_3}; \quad (16)$$

$$\psi_{h,x}^{phys} = e^{\frac{i}{2}\bar{\omega}_h\gamma_5\tau_1}\psi_{h,x}, \quad \bar{\psi}_{h,x}^{phys} = \bar{\psi}_{h,x}e^{\frac{i}{2}\bar{\omega}_h\gamma_5\tau_1}. \quad (17)$$

Since the simulations are usually performed near *full twist* corresponding to $\omega_l = \omega_h = \frac{\pi}{2}$, the modified twist angles are close to zero:

$$\bar{\omega}_l \simeq 0, \quad \bar{\omega}_h \simeq 0. \quad (18)$$

Therefore, near full twist the ψ -fields are approximately equal to the physical quark fields. At full twist the use of the ψ -basis is advantageous because the formulas are simpler than in the χ -basis.

The definition of the twist angles is not unique. There are different viable possibilities to define them and the *critical hopping parameters* corresponding to them (see, for instance, [21], [12], [22], [8], [23], [24], [25]).

Here, for the light doublet, we use the definition based on the requirement of parity conservation for some matrix element of the physical vector and axialvector current, as first introduced in [21], [12] and numerically studied in detail in [14]. For this let us introduce the bare vector- and axialvector bilinears

$$V_{l,x\mu}^a \equiv \bar{\chi}_{l,x}\frac{1}{2}\tau_a\gamma_\mu\chi_{l,x}, \quad A_{l,x\mu}^a \equiv \bar{\chi}_{l,x}\frac{1}{2}\tau_a\gamma_\mu\gamma_5\chi_{l,x} \quad (a = 1, 2). \quad (19)$$

The twist angle is introduced as the chiral rotation angle between the renormalised (physical) chiral currents:

$$\hat{V}_{l,x\mu}^a = Z_{lV}V_{l,x\mu}^a \cos \omega_l + \epsilon_{ab}Z_{lA}A_{l,x\mu}^b \sin \omega_l, \quad (20)$$

$$\hat{A}_{l,x\mu}^a = Z_{lA}A_{l,x\mu}^a \cos \omega_l + \epsilon_{ab}Z_{lV}V_{l,x\mu}^b \sin \omega_l \quad (21)$$

where only charged currents are considered ($a=1,2$), ϵ_{ab} is the antisymmetric unit tensor and Z_{lV} and Z_{lA} are the multiplicative renormalisation factors of the vector

and axialvector current, respectively. The exact requirements defining ω_l (and also yielding the value of Z_{lA}/Z_{lV}) is taken to be

$$\langle 0 | \hat{V}_{l,x,\mu=0}^+ | \pi^- \rangle = 0 , \quad \langle 0 | \hat{A}_{l,x,\mu=1,2,3}^+ | \rho^- \rangle = 0 . \quad (22)$$

For the heavy doublet, in principle, one could translate and use this construction, too, but for applications in the kaon and D-meson sector it is more natural to consider bilinears between the light and the heavy doublet. In addition, inside the heavy doublet, due to the off-diagonal twist, one also would have to consider disconnected quark contributions which are absent in the light-heavy sector. Let us introduce the bare vector-, axialvector-, scalar- and pseudoscalar bilinears in the K^+ - and D^0 -sector as

$$V_{K^+,x\mu} \equiv \bar{\chi}_{s,x} \gamma_\mu \chi_{u,x} , \quad A_{K^+,x\mu} \equiv \bar{\chi}_{s,x} \gamma_\mu \gamma_5 \chi_{u,x} , \quad (23)$$

$$S_{K^+,x} \equiv \bar{\chi}_{s,x} \chi_{u,x} , \quad P_{K^+,x} \equiv \bar{\chi}_{s,x} \gamma_5 \chi_{u,x} , \quad (24)$$

$$V_{D^0,x\mu} \equiv \bar{\chi}_{c,x} \gamma_\mu \chi_{u,x} , \quad A_{D^0,x\mu} \equiv \bar{\chi}_{c,x} \gamma_\mu \gamma_5 \chi_{u,x} , \quad (25)$$

$$S_{D^0,x} \equiv \bar{\chi}_{c,x} \chi_{u,x} , \quad P_{D^0,x} \equiv \bar{\chi}_{c,x} \gamma_5 \chi_{u,x} , \quad (26)$$

and similarly for the K^0 - and D^- -sector by changing $u \rightarrow d$. Denoting the kaon- and D-meson-doublet by $K \equiv (K^+ \ K^0)$ and $D \equiv (D^0 \ D^-)$, respectively, and introducing $\check{K} \equiv (K^+ \ -K^0)$ and $\check{D} \equiv (D^0 \ -D^-)$, the renormalised vector and axialvector currents of the kaon doublet are given by

$$\begin{aligned} \hat{V}_{K,x\mu} = & \cos \frac{\omega_l}{2} \cos \frac{\omega_h}{2} Z_V V_{K,x\mu} + \sin \frac{\omega_l}{2} \sin \frac{\omega_h}{2} Z_V V_{\check{D},x\mu} \\ & + i \sin \frac{\omega_l}{2} \cos \frac{\omega_h}{2} Z_A A_{\check{K},x\mu} - i \cos \frac{\omega_l}{2} \sin \frac{\omega_h}{2} Z_A A_{D,x\mu} , \end{aligned} \quad (27)$$

$$\begin{aligned} \hat{A}_{K,x\mu} = & \cos \frac{\omega_l}{2} \cos \frac{\omega_h}{2} Z_A A_{K,x\mu} + \sin \frac{\omega_l}{2} \sin \frac{\omega_h}{2} Z_A A_{\check{D},x\mu} \\ & + i \sin \frac{\omega_l}{2} \cos \frac{\omega_h}{2} Z_V V_{\check{K},x\mu} - i \cos \frac{\omega_l}{2} \sin \frac{\omega_h}{2} Z_V V_{D,x\mu} . \end{aligned} \quad (28)$$

Analogously for the scalar bilinears:

$$\begin{aligned} \hat{S}_{K,x} = & \cos \frac{\omega_l}{2} \cos \frac{\omega_h}{2} Z_S S_{K,x} - \sin \frac{\omega_l}{2} \sin \frac{\omega_h}{2} Z_S S_{\check{D},x} \\ & + i \sin \frac{\omega_l}{2} \cos \frac{\omega_h}{2} Z_P P_{\check{K},x} + i \cos \frac{\omega_l}{2} \sin \frac{\omega_h}{2} Z_P P_{D,x} , \end{aligned} \quad (29)$$

$$\begin{aligned} \hat{P}_{K,x} = & \cos \frac{\omega_l}{2} \cos \frac{\omega_h}{2} Z_P P_{K,x} - \sin \frac{\omega_l}{2} \sin \frac{\omega_h}{2} Z_P P_{\check{D},x} \\ & + i \sin \frac{\omega_l}{2} \cos \frac{\omega_h}{2} Z_S S_{\check{K},x} + i \cos \frac{\omega_l}{2} \sin \frac{\omega_h}{2} Z_S S_{D,x} . \end{aligned} \quad (30)$$

Similar relations hold in the D-meson doublet, too. (27)-(28) show that near full twist $\omega_{l,h} \simeq \pi/2$ all four terms on the right hand sides have roughly equal coefficients.

The requirement of parity symmetry in the isotriplets (pions, rho-mesons) allows to fix the twist angle ω_l , cf. (22). In the case of the heavy-light isodoublet one has to take into account the mixing between the kaons and D-mesons. In this case the twist angle ω_h (and ω_l) can be fixed by requiring conservation of parity and/or flavour symmetry.

The equations in (22) follow by considering [21], [12], [14] the (vanishing) vector-current-pseudoscalar and axialvector-current-vector-current correlators, which turns out to be the most convenient choice for fixing the twist angle in the light sector. In the heavy-light sector the mixing patterns for currents and scalar bilinears are similar, so any combination of operators gives similar expressions. However, correlators only made up of scalar bilinears are expected to give a better signal, so we concentrate on this case for the discussion. Considering the upper components, four bilinears P_{K+} , P_{D^0} , S_{K+} , S_{D^0} and the respective charge-conjugated versions must be included in the analysis. We define a four-dimensional vector of the multiplicatively renormalised bilinears

$$\mathcal{V} = \begin{pmatrix} Z_P P_{K+} \\ Z_P P_{D^0} \\ Z_S S_{K+} \\ Z_S S_{D^0} \end{pmatrix} \quad \bar{\mathcal{V}} = (-Z_P P_{K-}, -Z_P P_{\bar{D}^0}, Z_S S_{K-}, Z_S S_{\bar{D}^0}) \quad (31)$$

and analogously the vector $\hat{\mathcal{V}}$ of the *fully* renormalised bilinears according to (29), (30) (and the analogous equations for the *D*-mesons). (29) and (30) can be then reformulated in a compact notation as

$$\hat{\mathcal{V}} = \mathcal{M} \mathcal{V}, \quad \bar{\hat{\mathcal{V}}} = \bar{\mathcal{V}} \mathcal{M}^{-1} \quad (32)$$

with the 4×4 matrix \mathcal{M} given by

$$\mathcal{M}(\omega_l, \omega_h) = \begin{pmatrix} \cos \frac{\omega_l}{2} \cos \frac{\omega_h}{2} & -\sin \frac{\omega_l}{2} \sin \frac{\omega_h}{2} & i \sin \frac{\omega_l}{2} \cos \frac{\omega_h}{2} & i \sin \frac{\omega_h}{2} \cos \frac{\omega_l}{2} \\ -\sin \frac{\omega_l}{2} \sin \frac{\omega_h}{2} & \cos \frac{\omega_l}{2} \cos \frac{\omega_h}{2} & i \sin \frac{\omega_h}{2} \cos \frac{\omega_l}{2} & i \sin \frac{\omega_l}{2} \cos \frac{\omega_h}{2} \\ i \sin \frac{\omega_l}{2} \cos \frac{\omega_h}{2} & i \sin \frac{\omega_h}{2} \cos \frac{\omega_l}{2} & \cos \frac{\omega_l}{2} \cos \frac{\omega_h}{2} & -\sin \frac{\omega_l}{2} \sin \frac{\omega_h}{2} \\ i \sin \frac{\omega_h}{2} \cos \frac{\omega_l}{2} & i \sin \frac{\omega_l}{2} \cos \frac{\omega_h}{2} & -\sin \frac{\omega_l}{2} \sin \frac{\omega_h}{2} & \cos \frac{\omega_l}{2} \cos \frac{\omega_h}{2} \end{pmatrix}. \quad (33)$$

\mathcal{M} is the unitary matrix describing the mixing pattern between the kaon and D-meson doublets. One can easily see that

$$\mathcal{M}^T = \mathcal{M} \quad \text{and} \quad \mathcal{M}^\dagger(\omega_l, \omega_h) = \mathcal{M}^*(\omega_l, \omega_h) = \mathcal{M}(-\omega_l, -\omega_h) = \mathcal{M}^{-1}(\omega_l, \omega_h). \quad (34)$$

(The last equality is expected since reversing the sign of the angles corresponds to the inverse chiral transformation). One can at this point define a *correlator matrix* in the kaon-D-meson sector by

$$\mathcal{C} = \langle \mathcal{V} \otimes \bar{\mathcal{V}} \rangle \quad (35)$$

(for example, $\mathcal{C}_{11} \equiv -Z_P^2 \langle P_{K^+} P_{K^-} \rangle$) and its fully renormalised version $\hat{\mathcal{C}} = \langle \hat{\mathcal{V}} \otimes \bar{\hat{\mathcal{V}}} \rangle$. One has

$$\hat{\mathcal{C}} = \mathcal{M}(\omega_l, \omega_h) \mathcal{C} \mathcal{M}^{-1}(\omega_l, \omega_h) , \quad (36)$$

$$\mathcal{C} = \mathcal{M}^{-1}(\omega_l, \omega_h) \hat{\mathcal{C}} \mathcal{M}(\omega_l, \omega_h) . \quad (37)$$

Restoration of parity- and flavour-symmetry implies that $\hat{\mathcal{C}}$ is a diagonal matrix with $\mathcal{M}(\omega_l, \omega_h)$ the matrix realizing the diagonalisation. The off-diagonal elements of the matrix equation (36) can be in principle used to determine the angles ω_l and ω_h , while the diagonal elements give the physical correlators from which e.g. the masses can be obtained. Of course, in general, parity and flavour can only be restored up to $\mathcal{O}(a)$ violations.

Taking also into account the residual discrete symmetries possessed by the action defined by (1) and (8)-(9), the only non-trivial conditions are obtained by imposing the vanishing of the flavour violating matrix elements $\hat{\mathcal{C}}_{12}$, $\hat{\mathcal{C}}_{34}$ and transposed. Defining for brevity $s_l = \sin \frac{\omega_l}{2}$, $s_h = \sin \frac{\omega_h}{2}$, $c_l = \cos \frac{\omega_l}{2}$, $c_h = \cos \frac{\omega_h}{2}$, the conditions are:

$$\begin{aligned} \hat{\mathcal{C}}_{12} + \hat{\mathcal{C}}_{21} &= \left[(c_l c_h)^2 + (s_l s_h)^2 \right] (\mathcal{C}_{12} + \mathcal{C}_{21}) + \left[(s_l c_h)^2 + (s_h c_l)^2 \right] (\mathcal{C}_{34} + \mathcal{C}_{43}) \\ &\quad - 2c_l c_h s_l s_h (\mathcal{C}_{11} + \mathcal{C}_{22} - \mathcal{C}_{33} - \mathcal{C}_{44}) + i s_h c_h (s_l^2 - c_l^2) (\mathcal{C}_{13} - \mathcal{C}_{31} + \mathcal{C}_{24} - \mathcal{C}_{42}) \\ &\quad + i s_l c_l (s_h^2 - c_h^2) (\mathcal{C}_{23} - \mathcal{C}_{32} + \mathcal{C}_{14} - \mathcal{C}_{41}) = 0 , \end{aligned} \quad (38)$$

$$\begin{aligned} \hat{\mathcal{C}}_{34} + \hat{\mathcal{C}}_{43} &= \left[(c_h s_l)^2 + (c_l s_h)^2 \right] (\mathcal{C}_{12} + \mathcal{C}_{21}) + \left[(c_l c_h)^2 + (s_l s_h)^2 \right] (\mathcal{C}_{34} + \mathcal{C}_{43}) \\ &\quad + 2c_l c_h s_l s_h (\mathcal{C}_{11} + \mathcal{C}_{22} - \mathcal{C}_{33} - \mathcal{C}_{44}) - i s_h c_h (s_l^2 - c_l^2) (\mathcal{C}_{13} - \mathcal{C}_{31} + \mathcal{C}_{24} - \mathcal{C}_{42}) \\ &\quad - i s_l c_l (s_h^2 - c_h^2) (\mathcal{C}_{23} - \mathcal{C}_{32} + \mathcal{C}_{14} - \mathcal{C}_{41}) = 0 . \end{aligned} \quad (39)$$

The sum of the two above equations implies

$$\mathcal{C}_{12} + \mathcal{C}_{21} + \mathcal{C}_{34} + \mathcal{C}_{43} = 0 . \quad (40)$$

A non trivial relation for the renormalisation constants of the bilinears is obtained from (40)

$$Z_P^2 / Z_S^2 = \frac{\langle S_{K^+} S_{\bar{D}^0} \rangle + \langle S_{D^0} S_{K^-} \rangle}{\langle P_{K^+} P_{\bar{D}^0} \rangle + \langle P_{D^0} P_{K^-} \rangle} , \quad (41)$$

which can be used for a non-perturbative determination of Z_P / Z_S .

Using (40), (38) (or (39)) can be restated in a compact way as a relation between $\cot \omega_h$ and $\cot \omega_l$

$$\cot \omega_h = \frac{\mathcal{C}_{11} + \mathcal{C}_{22} - \mathcal{C}_{33} - \mathcal{C}_{44} + i(\mathcal{C}_{13} - \mathcal{C}_{31} + \mathcal{C}_{24} - \mathcal{C}_{42}) \cot \omega_l}{(\mathcal{C}_{12} + \mathcal{C}_{21} - \mathcal{C}_{34} - \mathcal{C}_{43}) \cot \omega_l - i(\mathcal{C}_{23} - \mathcal{C}_{32} + \mathcal{C}_{14} - \mathcal{C}_{41})} . \quad (42)$$

This can be used to determine ω_h once ω_l is known. (ω_l can be obtained following the prescription of [21], [12], [14]).

This discussion suggests that, especially near full twist where the mixing is maximal, the analysis of the masses in the kaon-D-meson sector should be performed by considering the 4-dimensional correlator matrix \mathcal{C} .

For tuning the hopping parameters the *untwisted PCAC quark mass* is also very useful. In the light doublet it is defined by the PCAC-relation containing the axialvector current $A_{l,x\mu}^a$ in (19) and the corresponding pseudoscalar density $P_{l,x}^a = \bar{\chi}_{l,x} \frac{1}{2} \tau_a \gamma_5 \chi_{l,x}$:

$$am_{\chi l}^{PCAC} \equiv \frac{\langle \partial_\mu^* A_{l,x\mu}^+ P_{l,y}^- \rangle}{2 \langle P_{l,x}^+ P_{l,y}^- \rangle} \quad (43)$$

where $\tau_\pm \equiv \tau_1 \pm i\tau_2$. The condition of full twist in the light quark sector obtained from (22) by setting $\omega_l = \pi/2$ coincides [14] with $m_{\chi l}^{PCAC} = 0$.

In the heavy sector one can define an untwisted PCAC quark mass $m_{\chi h}^{PCAC}$, too. A natural definition is obtained by considering the axialvector Ward identity

$$\partial_\mu^* A_{h,x\mu}^a = 2am_{\chi h}^{PCAC} P_{h,x}^a + \begin{cases} 2iZ_A^{-1} a\mu_\sigma S_{h,x}^0, & a = 1 \\ 0, & a = 2 \\ (-2i)Z_A^{-1} a\mu_\delta P_{h,x}^0, & a = 3 \end{cases} \quad (44)$$

where, in analogy with the light sector in (19), we define

$$A_{h,x\mu}^a \equiv \bar{\chi}_{h,x} \frac{1}{2} \tau_a \gamma_\mu \gamma_5 \chi_{h,x} \quad (a = 1, 2, 3), \quad S_{h,x}^0 \equiv \bar{\chi}_{h,x} \chi_{h,x}, \quad P_{h,x}^0 \equiv \bar{\chi}_{h,x} \gamma_5 \chi_{h,x}. \quad (45)$$

(Observe that for uniformity with the definition (43) we incorporate a factor Z_A^{-1} in the definition of the untwisted PCAC quark mass). The above identity could in principle be used to tune ω_h to $\pi/2$ by imposing $am_{\chi h}^{PCAC} = 0$. However, as already mentioned, the presence of disconnected contributions in the heavy sector are likely not to allow for precise determinations.

One can consider also in this case the heavy-light sector. Here the axialvector Ward identities read

$$\partial_\mu^* A_{K,x\mu} = (am_{\chi s}^{PCAC} + am_{\chi l}^{PCAC}) P_{K,x\mu} + iZ_A^{-1} a\mu_l S_{\check{K},x\mu} + iZ_A^{-1} a\mu_\sigma S_{D,x\mu} \quad (46)$$

$$\partial_\mu^* A_{D,x\mu} = (am_{\chi c}^{PCAC} + am_{\chi l}^{PCAC}) P_{D,x\mu} + iZ_A^{-1} a\mu_l S_{\check{D},x\mu} + iZ_A^{-1} a\mu_\sigma S_{K,x\mu}. \quad (47)$$

The solution of the over-determined linear system, obtained by taking a suitable matrix element (for instance, $\langle \partial_\mu^* A_{K^+,x\mu} P_{K^-,y} \rangle$), allows to determine numerically (together with (43)) the untwisted PCAC mass of the heavy quarks $m_{\chi c}^{PCAC}$, $m_{\chi s}^{PCAC}$ and the renormalisation factor Z_A . The condition of full twist in the heavy doublet can be written as

$$m_{\chi h}^{PCAC} \equiv m_{\chi c}^{PCAC} + m_{\chi s}^{PCAC} = 0. \quad (48)$$

The quark masses defined by (43) and (46)-(47) are untwisted components of bare quark masses. The physical quark masses can be obtained by the corresponding PCAC-

relations of the renormalised currents and densities:

$$am_l^{PCAC} \equiv \frac{\langle \partial_\mu^* \hat{A}_{l,x\mu}^+ \hat{P}_{l,y}^- \rangle}{2 \langle \hat{P}_{l,x}^+ \hat{P}_{l,y}^- \rangle}, \quad (49)$$

$$am_s^{PCAC} + am_l^{PCAC} \equiv \frac{\langle \partial_\mu^* \hat{A}_{K^+,x\mu} \hat{P}_{K^-,y} \rangle}{\langle \hat{P}_{K^+,x} \hat{P}_{K^-,y} \rangle}, \quad (50)$$

$$am_c^{PCAC} + am_l^{PCAC} \equiv \frac{\langle \partial_\mu^* \hat{A}_{D^+,x\mu} \hat{P}_{D^-,y} \rangle}{\langle \hat{P}_{D^+,x} \hat{P}_{D^-,y} \rangle}. \quad (51)$$

They are related to the bare quark masses by

$$m_l^{PCAC} = Z_P^{-1} \sqrt{(Z_A m_{\chi^l}^{PCAC})^2 + \mu_l^2}, \quad (52)$$

$$m_{c,s}^{PCAC} = Z_P^{-1} \sqrt{(Z_A m_{\chi^h}^{PCAC})^2 + \mu_\sigma^2} \pm Z_S^{-1} \mu_\delta. \quad (53)$$

4 Numerical simulations

Our main goal in this work is to gain experience with the tuning of lattice parameters for future large scale simulations. Based on our recent work with $N_f = 2$ dynamical twisted mass Wilson fermion QCD simulations in Refs. [11], [12], [13], [14] and [26], the main emphasis is on the effects of the additional dynamical flavours s and c . As in the $N_f = 2$ case, we start with coarse lattices: lattice spacings about $a \simeq 0.2$ fm on a $12^3 \cdot 24$ lattice and $a \simeq 0.15$ fm on a $16^3 \cdot 32$ lattice. (This implies spatial lattice extensions of $L \simeq 2.4$ fm.) The parameters of our main runs are: on the $12^3 \cdot 24$ lattice $\beta = 3.25$, $a\mu_l = 0.01$, $a\mu_\sigma = 0.315$, $a\mu_\delta = 0.285$ and on the $16^3 \cdot 32$ lattice $\beta = 3.35$, $a\mu_l = 0.0075$, $a\mu_\sigma = 0.2363$, $a\mu_\delta = 0.2138$. The statistics is between 500 and 1100 PHMC trajectories of length 0.4. (Of course, in order to find the appropriate parameters, we also had to perform at the beginning several additional short runs which we do not include here.)

The tuning to full twist of the theory with an additional heavy doublet is complicated by the fact that *two* independent parameters κ_l and κ_h must be set to their respective critical values, using e.g. for the heavy sector the procedure outlined in the previous section. However, it can be shown that in the continuum limit the deviation of the two critical hopping parameters $\kappa_{l,cr}$ and $\kappa_{h,cr}$ goes to zero as $\mathcal{O}(a)$. An argument is given in the Appendix. This suggests to tune κ_l to the value where $m_{\chi^l}^{PCAC} = 0$ with $\kappa_h = \kappa_l$: in this situation $m_{\chi^h}^{PCAC} = \mathcal{O}(a)$. Observe that since the average quark mass in the heavy sector is typically large, the $\mathcal{O}(a)$ error is expected not to affect the full twist improvement in the sense of [6], while it is critical to have good tuning in the light quark sector. This can be checked by computing ω_h as suggested in the previous section and verifying $\omega_h \approx \pi/2$.

In view of this, we have set the two hopping parameters to be equal in our main runs: $\kappa \equiv \kappa_l = \kappa_h$. (In a few additional runs we checked that small individual changes of κ_h by $\Delta\kappa_h \simeq 0.001$ do not alter any of the qualitative conclusions.)

The average plaquette values as a function of the hopping parameter $\kappa_l = \kappa_h = \kappa$, for fixed values of the twisted masses, are shown by Figures 1 and 2 on the $12^3 \cdot 24$ and $16^3 \cdot 32$ lattices, respectively. On the $12^3 \cdot 24$ lattice a strong metastability is observed for $0.1745 \leq \kappa \leq 0.1747$, which we interpret as the manifestation of a *first order phase transition*. This behaviour agrees with one of the scenarios predicted by ChPT including leading lattice artifacts [27], [28], [29], [30]. It has also been observed in our previous simulations, for instance, in [11]. On the $16^3 \cdot 32$ lattice no metastability could be observed, although there is a sharp rise of the average plaquette value between $\kappa = 0.1705$ and $\kappa = 0.1706$. This may also signal a (weaker) first order phase transition or a *cross-over*. To decide among these two possibilities, in principle, an investigation of the infinite volume behaviour would be necessary. In practice, in a finite volume, the effects of a real first order phase transition and a cross-over are similar.

We emphasize that this observed behaviour is not related to some imperfection of the simulation algorithm. Due to the positive twisted masses the eigenvalues of the fermion matrix have a positive lower bound. Therefore, we could choose the HMC step size small enough in order that the molecular dynamical force does not become too large. The behaviour of the system when crossing the phase transition region is nicely illustrated by the run history in Figure 3. One can recognize three stages in the plot: metastable start at $m_{\chi_l}^{PCAC} > 0$; crossing; stable thermalization at $m_{\chi_l}^{PCAC} < 0$. A high concentration of small eigenvalues occurs during the crossing, because a large portion of the Dirac spectrum (actually all the physically relevant eigenvalues) is moving from the right half complex plane with $\text{Re}\lambda > 0$ to the left one with $\text{Re}\lambda < 0$.

We determined several quantities in both the pion- and kaon-sector. The values of some of them are collected in Tables 2 and 3. As in our previous work, we determined the lattice spacing from the quark force by the Sommer scale parameter [31] assuming $r_0 \equiv 0.5 \text{ fm}$. Taking the values for positive untwisted PCAC quark masses ($am_{\chi_l}^{PCAC} > 0$), we get for $\beta = 3.25$ on the $12^3 \cdot 24$ lattice $a(\beta = 3.25) \simeq 0.20 \text{ fm}$ and for $\beta = 3.35$ on the $16^3 \cdot 32$ lattice $a(\beta = 3.35) \simeq 0.15 \text{ fm}$. These correspond to $a^{-1} \simeq 1.0 \text{ GeV}$ and $a^{-1} \simeq 1.3 \text{ GeV}$, respectively.

It follows from the data in Tables 2 and 3 that the pion, and hence the u - and d -quark masses, are not particularly small in our runs. Considering only the points with positive untwisted PCAC quark mass ($am_{\chi_l}^{PCAC} > 0$) outside the metastability region at $\beta = 3.25$ we have $m_\pi \geq 670 \text{ MeV}$. At $\beta = 3.35$ the corresponding value is $m_\pi \geq 450 \text{ MeV}$. (The points with $am_{\chi_l}^{PCAC} < 0$ have $m_\pi \geq 530 \text{ MeV}$ and $m_\pi \geq 560 \text{ MeV}$ for the two β -values, respectively, but they are usually not considered for large scale simulations because of the strongly fluctuating small eigenvalues as shown,

for instance, by Fig. 3.)

The kaon masses are also given Tables 2 and 3. Let us note that, in the Frezzotti-Rossi formulation of the split-mass doublet we use, the masses in the kaon doublet (and D-meson doublet) are exactly degenerate. This follows from an exact symmetry of the lattice action defined in Section 2.1 (both in the χ - and ψ -basis of quark fields) namely, simultaneous multiplication by an isospin matrix and space reflection:

$$S : \begin{cases} \text{light: Parity} \otimes \tau_1 : \begin{cases} u(x) \rightarrow \gamma_0 d(x_P) \\ d(x) \rightarrow \gamma_0 u(x_P) \end{cases} \\ \text{heavy: Parity} \otimes \tau_3 : \begin{cases} c(x) \rightarrow \gamma_0 c(x_P) \\ s(x) \rightarrow -\gamma_0 s(x_P) \end{cases} \end{cases} \quad (54)$$

This *exact* symmetry exchanges the u -quark and the d -quark, hence the equality of the masses within kaon- and D-meson doublets follows.

Let us note that in a recent publication [32] a non-zero kaon mass splitting has been calculated in the quenched approximation using another formulation [33] of the mass-split doublet where both the twist and the mass splitting are in the same isospin direction. This formulation has, however, the disadvantage that the fermion determinant is non-real and therefore an unquenched computation is practically impossible at present. The difference in the presence and absence of the kaon mass splitting in the two formulations comes from the fact that the states with a given quark flavour correspond to different linear combinations here and there.

Similarly to the pion masses, the kaon masses in Tables 2 and 3 are also higher than the physical value. In the points cited above for the pion mass we have: at $\beta = 3.25$ and $\beta = 3.35$ $m_K \geq 920$ MeV and $m_K \geq 850$ MeV, respectively. The kaon mass can be easily lowered by tuning the mass parameters in the heavy doublet. In order to explore this we also performed simulations at $\beta = 3.35$, $a\mu_l = 0.0075$ on the $16^3 \cdot 32$ lattice with $a\mu_\sigma = a\mu_\delta = 0.15$. For instance, at $\kappa_l = \kappa_h = 0.17$ we got $am_\pi = 0.4432(40)$ and $am_K = 0.5918(22)$. Comparing to the third line in Table 3 one can see that both the pion and the kaon mass become smaller. In particular, the kaon mass is smaller by a factor of about $3/4$. This shows that the kaon mass can probably be tuned to its physical value if wanted. Another possibility is to do the chiral extrapolation by fixing, instead of m_K , the pion-kaon mass ratio m_π/m_K to its physical value.

The D-meson masses in Tables 2 and 3 are typically smaller than the physical value. In the points cited above for the pion and kaon masses we have: at $\beta = 3.25$ and $\beta = 3.35$ $m_D \simeq 1450$ MeV and $m_D \simeq 1400$ MeV, respectively. m_D can, in principle, also be tuned to its physical value. However, on coarse lattices the D-meson mass is close to the cut-off and, therefore, it is more reasonable to keep it smaller than the physical value in order to be well below the cut-off. In fact, in our runs the actual D-meson masses are already at the cut-off because we have $a^{-1} \simeq 1$ GeV and

$a^{-1} \simeq 1.3 \text{ GeV}$ at $\beta = 3.25$ and $\beta = 3.35$, respectively. But on a fine lattice, say with $a^{-1} \simeq 4 \text{ GeV}$, it will become possible to directly go to the physical value of m_D , too.

The machinery for the twist angle in the heavy doublet ω_h developed in Sec. 3 has been tested in a few runs, too. The formulas worked fine and the results turned out to be plausible. For instance, in the run at $\beta = 3.35$, $\kappa_l = \kappa_h = 0.1704$, $a\mu_l = 0.0075$, $a\mu_\sigma = 0.2363$, $a\mu_\delta = 0.2138$ on a $16^3 \cdot 32$ lattice we obtained from 400 gauge configurations:

$$\begin{aligned} \omega_l/\pi &= 0.0981(55), & \omega_h/\pi &= 0.490(25), \\ Z_P/Z_S &= 0.5739(65), & Z_A &= 0.897(11), & Z_V &= 0.5490(12). \end{aligned} \quad (55)$$

As one sees, ω_h is rather close to $\pi/2$ even if ω_l is still far from it. This is a consequence of $\mu_\sigma \gg \mu_l$. Using the relation (valid in the continuum) $\cot(\omega_h)/\cot(\omega_l) = \mu_l/\mu_\sigma$ and the value of ω_l given above, one would get $\omega_h/\pi = 0.468$. The situation is very similar in the runs on a $12^3 \cdot 24$ lattice, too. For instance, in the run with largest untwisted mass of Table 2 at $\kappa_l = \kappa_h = 0.1740_L$ we obtained:

$$\omega_l/\pi = 0.04298(34), \quad \omega_h/\pi = 0.4356(83), \quad Z_P/Z_S = 0.581(11). \quad (56)$$

These results imply that putting the untwisted quark mass equal in the two sectors gives an elegant solution for tuning to full twist: one can just do the same as in the $N_f = 2$ case. Due to the large twisted component in the heavy sector, the tuning of ω_h to $\pi/2$ is no problem at all: already at moderate values of ω_l , ω_h is almost equal to $\pi/2$.

Let us finally mention that using Chiral Perturbation Theory (ChPT) formulas one can also extrapolate from our simulation points to smaller pion- and kaon-masses. As a simple example, let us take the squared pion-kaon mass ratio in lowest order (LO) ChPT:

$$(m_\pi/m_K)^2 = \frac{2m_{ud}}{m_{ud} + m_s}. \quad (57)$$

In terms of our parameters we can set

$$m_{ud} = \sqrt{(Z_A m_{\chi^l}^{PCAC})^2 + \mu_l^2}, \quad m_s = \sqrt{(Z_A m_{\chi^h}^{PCAC})^2 + (\mu_\sigma)^2} - \frac{Z_P}{Z_S} \mu_\delta \quad (58)$$

where Z_P/Z_S is a fitted relative renormalisation factor. In our fits we set, for simplicity, $Z_A = 0.897$ from (55) and we also assumed $m_{\chi^h}^{PCAC} = m_{\chi^l}^{PCAC}$, which corresponds to the assumption $\kappa_{h,cr} = \kappa_{l,cr}$. The results for both β values are shown in Figure 6. Note that although these fits look rather good, clearly, the validity of Chiral Perturbation Theory in general has to be checked in further simulations at small values of a and m_π .

It turns out that the fitted values of Z_P/Z_S are well below 1, namely $Z_P/Z_S \simeq 0.45$, which implies that, as also directly shown by our simulation data, the kaon mass reacts

relatively weakly to the change of the bare quark mass difference parameter $a\mu_\delta$. The deviation of Z_P/Z_S obtained in the LO-ChPT fit from the values in (55) and (56) might be due to lattice artifacts or/and to the fact that in (55)-(56) no extrapolation to zero quark masses is performed.

Note that the obtained values of Z_P/Z_S do not satisfy the bound derived in [4] which would ensure the positivity of the quark determinant, because in case of the (c, s) -doublet this bound is $Z_P/Z_S > (m_c - m_s)/(m_c + m_s) \simeq 0.85$. This means that there might be some gauge configuration where the determinant of the (c, s) -doublet is negative. However, such configurations have a very low probability and hence they practically never occur in Monte Carlo simulations. This is shown by the eigenvalues of the fermion matrix which never come close to zero: for the (c, s) -doublet in our simulations they always satisfy $\lambda_{min,h} > 0.01$. (This has to be compared to the minimal eigenvalues in the (u, d) -doublet which only satisfy $\lambda_{min,l} > 0.0001$.)

It is remarkable that the minimum value of the interpolated curves in Figure 6 are not far away from the physical value $(m_\pi/m_K)^2 \simeq 0.082$. This raises the interesting question, whether it would be possible to perform unconventional chiral extrapolations from simulation data at fixed twisted masses.

5 Discussion

The main conclusion of the present paper is that numerical simulations of QCD with unquenched u , d , s and c quarks are possible in the twisted-mass Wilson formulation.

The PHMC updating algorithm with multi-step polynomial approximations and stochastic correction during the update turned out to be effective even in difficult situations near a first order phase transition (or cross-over). The autocorrelations of the quantities given in Tables 2 and 3 are typically of $\mathcal{O}(1)$ in number of PHMC-trajectories (most of the time of length 0.4), therefore, it is worth to analyse the gauge configurations after every trajectory.

At $\beta = 3.25$ (lattice spacing $a \simeq 0.20$ fm) on our $12^3 \cdot 24$ lattice we observed strong metastabilities suggesting a first order phase transition. This agrees with one of the scenarios predicted by ChPT including leading lattice artifacts [27], [28], [29], [30] and has been observed previously in several QCD simulations with Wilson fermions [34], [35], [36], [11]. At $\beta = 3.35$ (lattice spacing $a \simeq 0.15$ fm) on our $16^3 \cdot 32$ lattice the phase transition becomes weaker but is still visible as a strong cross-over region with fast changes in several quantities. Compared to $N_f = 2$ runs at similar lattice spacings the first order phase transition becomes stronger for $N_f = 2 + 1 + 1$. (This agrees with the early observations in [35].)

The smallest simulated pion mass in a stable point with positive untwisted PCAC quark mass ($am_{\chi_l}^{PCAC} > 0$) at $\beta = 3.25$ ($a \simeq 0.20$ fm) and $\beta = 3.35$ ($a \simeq 0.15$ fm) is

$m_\pi \simeq 670 \text{ MeV}$ and $m_\pi \simeq 450 \text{ MeV}$, respectively. Our expectation based on the ChPT formulas and on our previous experience is that, for instance, on a $24^3 \cdot 48$ lattice with $a \simeq 0.10 \text{ fm}$ the minimal pion mass at $a\mu = 0.005$ will be somewhere in the range $270 \text{ MeV} < m_\pi^{min} < 300 \text{ MeV}$. This is because at vanishing twisted masses m_π^{min} is going to zero as $\mathcal{O}(a)$ and for positive twisted mass the decrease is somewhat faster. (The lower value of the estimate corresponds to the minimum of the extrapolated curve in Figure 6.)

The kaon mass in the present simulations is higher than the physical value but can probably be properly tuned by changing the twisted mass parameters in the c - s doublet. The D-meson mass is smaller than the physical value (i.e. the c - s mass splitting is smaller than in nature) but this is reasonable on coarse lattices in order to stay with it below the cut-off. On finer lattices (say, with $a \simeq 0.05 \text{ fm}$) one can try to tune also the D-meson mass to its physical value. A possible difficulty in properly tuning the mass splittings in the c - s doublet can be caused by the relative insensitivity of the masses to the bare mass-splitting parameter $a\mu_\delta$. This may imply the necessity of some extrapolations in the mass ratios.

In case of the c - s -doublet the mass splitting is rather large because the renormalised quark masses satisfy $(m_c - m_s)/(m_c + m_s) \simeq 0.85$. Therefore it is important to take into account the mass splitting. For the u - d -doublet, well above the scale of u and d quark masses, the mass degeneracy can be considered as a good approximation, but even in this case we have in nature $(m_d - m_u)/(m_d + m_u) \simeq 0.28$. Hence also there, on a long run, the problem of the quark mass splitting within the doublet has to be tackled.

In summary, our experience in this paper is rather positive both for the twisted-mass Wilson fermion formulation and for the PHMC algorithm we are using. This opens the road for future large scale QCD simulations with dynamical u , d , s and c quarks.

Acknowledgments

We acknowledge helpful discussions with Roberto Frezzotti, Andrea Shindler and Urs Wenger. We thank the computer centers at DESY Hamburg and NIC at Forschungszentrum Jülich for providing us the necessary technical help and computer resources. This research has been supported by the DFG Sonderforschungsbereich/Transregio SFB/TR9-03 and in part by the EU Integrated Infrastructure Initiative Hadron Physics (I3HP) under contract RII3-CT-2004-506078 and also in part by the U.S. Department of Energy under contract number DE-AC02-98CH10886. The work of T.C. is supported by the DFG in the form of a Forschungsstipendium CH 398/1.

Appendix

In the $N_f = 2$ theory, one possible definition of the critical quark mass $m_{0cr}(g_0, \mu)$ is given by the vanishing of the PCAC quark mass m_χ^{PCAC} . Due to chirality breaking the latter gets shifted:

$$m_\chi^{PCAC} = m_0 - a^{-1}f(g_0, am_0, a\mu) , \quad (59)$$

with f a dimensionless function. On the basis of the symmetry of the action under parity $\times (\mu \rightarrow -\mu)$ one can show that the additive renormalisation of the quark mass is *even* in μ , and analyticity in turn implies

$$f(g_0, am_0, a\mu) = f(g_0, am_0) + \mathcal{O}(\mu^2 a^2) , \quad (60)$$

where $f(g_0, am_0)$ is the shift for ordinary $N_f = 2$ QCD without twisted mass term. So the twisted mass term in the action only produces an $\mathcal{O}(a)$ effect on the quark mass (with g_0 and m_0 held fixed):

$$m_\chi^{PCAC} = m_0 - a^{-1}f(g_0, am_0) + \mathcal{O}(a) . \quad (61)$$

The above argument can be easily generalized to the $N_f = 2 + 1 + 1$ theory. Here one has to make a distinction between the two sectors:

$$m_{\chi l}^{PCAC} = m_{0l} - a^{-1}f_l(g_0, am_{0l}, am_{0h}, a\mu_l, a\mu_\sigma, a\mu_\delta) , \quad (62)$$

$$m_{\chi h}^{PCAC} = m_{0h} - a^{-1}f_h(g_0, am_{0h}, am_{0l}, a\mu_\sigma, a\mu_l, a\mu_\delta) . \quad (63)$$

The functions f_l and f_h are in this case even in μ_l , μ_h and μ_δ ¹: similarly to $N_f = 2$, the associated terms in the action only affect the additive renormalisation of the quark mass by $\mathcal{O}(a)$ terms. So we write:

$$m_{\chi l}^{PCAC} = m_{0l} - a^{-1}f(g_0, am_{0l}, am_{0h}) + \mathcal{O}(a) , \quad (64)$$

$$m_{\chi h}^{PCAC} = m_{0h} - a^{-1}f(g_0, am_{0h}, am_{0l}) + \mathcal{O}(a) , \quad (65)$$

where on the r.h.s. we have now the mass-shifts for the theory without twist and mass-splitting ($N_f = 2 + 2$ QCD): here the distinction between the two sectors is immaterial. From eqs. (64), (65) it follows immediately

$$m_{0l} = m_{0h} = m_0 \quad \Rightarrow \quad m_{\chi h}^{PCAC} = m_{\chi l}^{PCAC} + \mathcal{O}(a) . \quad (66)$$

¹An additional symmetry in the heavy sector is needed for the argument, namely $\chi_{h,x} \rightarrow \exp\{i\frac{\pi}{2}\tau_1\}\chi_{h,x}$, $\bar{\chi}_{h,x} \rightarrow \chi_{h,x} \exp\{-i\frac{\pi}{2}\tau_1\}$ composed with $\mu_\delta \rightarrow -\mu_\delta$.

References

- [1] Fermilab Lattice, MILC and HPQCD Collaboration, A.S. Kronfeld et al., PoS LAT2005 (2005) 206, Int. J. Mod. Phys. **A21** (2006) 713; hep-lat/0509169.
- [2] JLQCD Collaborations, CP-PACS et al., PoS LAT2005 (2005) 057; hep-lat/0509142.
- [3] R. Frezzotti, P. A. Grassi, S. Sint and P. Weisz, Nucl. Phys. Proc. Suppl. **83** (2000) 941; hep-lat/9909003.
- [4] R. Frezzotti and G.C. Rossi, Nucl. Phys. Proc. Suppl. **128** (2004) 193; hep-lat/0311008.
- [5] F. Farchioni *et al.*, PoS **LAT2005** (2005) 072; hep-lat/0509131.
- [6] R. Frezzotti and G.C. Rossi, JHEP **0408** (2004) 007; hep-lat/0306014; Nucl. Phys. Proc. Suppl. **129** (2004) 880; hep-lat/0309157.
- [7] K. Jansen, A. Shindler, C. Urbach and I. Wetzorke [XLF Collaboration], Phys. Lett. B **586** (2004) 432; hep-lat/0312013.
- [8] W. Bietenholz *et al.* [XLF Collaboration], JHEP **0412** (2004) 044; arXiv:hep-lat/0411001.
- [9] K. Jansen, M. Papinutto, A. Shindler, C. Urbach and I. Wetzorke [XLF Collaboration], Phys. Lett. B **619** (2005) 184; hep-lat/0503031.
- [10] K. Jansen, M. Papinutto, A. Shindler, C. Urbach and I. Wetzorke [XLF Collaboration], JHEP **0509** (2005) 071; hep-lat/0507010.
- [11] F. Farchioni *et al.*, Eur. Phys. J. C **39** (2005) 421; hep-lat/0406039.
- [12] F. Farchioni *et al.*, Eur. Phys. J. C **42** (2005) 73; hep-lat/0410031.
- [13] F. Farchioni *et al.*, Phys. Lett. B **624** (2005) 324; hep-lat/0506025.
- [14] F. Farchioni *et al.*, Eur. Phys. J. C (2006), DOI 10.1140/epjc/s2006-02549-y; hep-lat/0512017.
- [15] K. Symanzik, Nucl. Phys. **B226** (1983) 187;
- [16] P. Weisz, Nucl. Phys. B **212** (1983) 1.
P. Weisz and R. Wohlert, Nucl. Phys. B **236** (1984) 397 [Erratum-ibid. B **247** (1984) 544].
- [17] I. Montvay and E. Scholz, Phys. Lett. B **623** (2005) 73; hep-lat/0506006.
- [18] R. Frezzotti and K. Jansen, Phys. Lett. B **402** (1997) 328; hep-lat/9702016;
R. Frezzotti and K. Jansen, Nucl. Phys. B **555** (1999) 395; hep-lat/9808011;
R. Frezzotti and K. Jansen, Nucl. Phys. B **555** (1999) 432; hep-lat/9808038.

- [19] I. Montvay, Nucl. Phys. B **466** (1996) 259; hep-lat/9510042.
- [20] T. Chiarappa, R. Frezzotti and C. Urbach, PoS **LAT2005** (2006) 103; hep-lat/0509154 and work in preparation.
- [21] F. Farchioni *et al.*, Nucl. Phys. Proc. Suppl. **140** (2005) 240; hep-lat/0409098.
- [22] S. Aoki and O. Bär, Phys. Rev. D **70** (2004) 116011; hep-lat/0409006;
S. Aoki and O. Bär, hep-lat/0604018.
- [23] S. R. Sharpe and J. M. S. Wu, Phys. Rev. D **71** (2005) 074501; hep-lat/0411021.
- [24] R. Frezzotti, G. Martinelli, M. Papinutto and G. C. Rossi, hep-lat/0503034.
- [25] S. R. Sharpe, Phys. Rev. D **72** (2005) 074510; hep-lat/0509009.
- [26] ETM Collaboration, in preparation.
- [27] S. R. Sharpe and R. L. Singleton, Phys. Rev. D **58** (1998) 074501; hep-lat/9804028.
- [28] G. Münster, JHEP **0409** (2004) 035; hep-lat/0407006.
- [29] L. Scorzato, Eur. Phys. J. C **37** (2004) 445; hep-lat/0407023.
- [30] S. R. Sharpe and J. M. S. Wu, Phys. Rev. D **70** (2004) 094029; hep-lat/0407025.
- [31] R. Sommer, Nucl. Phys. B **411** (1994) 839; hep-lat/9310022.
- [32] A. M. Abdel-Rehim, R. Lewis, R. M. Woloshyn and J. M. S. Wu, hep-lat/0601036.
- [33] C. Pena, S. Sint and A. Vladikas, JHEP **0409** (2004) 069; hep-lat/0405028.
- [34] T. Blum *et al.*, Phys. Rev. D **50** (1994) 3377; hep-lat/9404006.
- [35] S. Aoki *et al.* [JLQCD Collaboration], Nucl. Phys. Proc. Suppl. **106** (2002) 263; hep-lat/0110088.
- [36] K. Jansen, Nucl. Phys. Proc. Suppl. **129** (2004) 3; hep-lat/0311039.

Tables

Table 1: *Algorithmic parameters in two runs on a $16^3 \cdot 32$ lattice at $\beta = 3.35$, $\kappa_l = \kappa_h = \kappa$, $a\mu_l = 0.0075$, $a\mu_\sigma = 0.2363$, $a\mu_\delta = 0.2138$ and with determinant break-up $n_B = 2$. The first line for a given κ shows the pion mass and the parameters for the light doublet, the second line the kaon mass and the parameters for the heavy doublet.*

κ	$am_{\pi,K}$	ϵ	λ	n_1	\bar{n}_1	n_2	\bar{n}_2
0.1690	0.8237(13)	1.25e-2	25	70	110	120	160
	0.9231(11)	3.25e-2	26	50	80	90	130
0.1705	0.3433(52)	1.875e-4	25	220	320	800	930
	0.6503(18)	1.875e-2	26	60	100	120	160

Table 2: *Selected results of the runs on a $12^3 \cdot 24$ lattice at $\beta = 3.25$, $a\mu_l = 0.01$, $a\mu_\sigma = 0.315$, $a\mu_\delta = 0.285$. The subscript on $\kappa = \kappa_l = \kappa_h$ denotes: L for “low” and H for “high” plaquette phase, respectively.*

$\kappa_l = \kappa_h$	r_0/a	am_π	am_ρ	am_K	am_D	$am_{\chi^l}^{PCAC}$
0.1740 _L	2.35(12)	0.7110(21)	0.9029(27)	0.9487(16)	1.4858(75)	0.08432(56)
0.1743 _L	2.279(56)	0.6718(59)	0.8756(30)	0.9277(22)	1.4543(99)	0.07515(45)
0.1745 _L	2.460(55)	0.5706(76)	0.7927(43)	0.8729(31)	1.4350(94)	0.0544(10)
0.1746 _L	2.489(54)	0.5616(47)	0.7891(33)	0.8700(19)	1.433(23)	0.05205(81)
0.1747 _L	2.457(48)	0.5303(74)	0.7566(75)	0.8566(38)	1.403(16)	0.04602(77)
0.1745 _H	3.840(81)	0.3991(86)	1.0635(84)	0.8232(27)	1.096(16)	-0.0260(15)
0.1746 _H	3.85(11)	0.481(11)	0.881(48)	0.8395(22)	1.055(37)	-0.0419(15)
0.1747 _H	3.98(11)	0.456(13)	0.996(36)	0.8375(26)	1.028(42)	-0.0403(23)
0.1750 _H	3.884(91)	0.531(18)	1.0936(97)	0.8690(46)	1.064(37)	-0.0525(24)
0.1755 _H	4.02(10)	0.7012(97)	1.1056(99)	0.9186(27)	1.219(41)	-0.0868(17)

Table 3: *Selected results of the runs on a $16^3 \cdot 32$ lattice at $\beta = 3.35$, $a\mu_l = 0.0075$, $a\mu_\sigma = 0.2363$, $a\mu_\delta = 0.2138$.*

$\kappa_l = \kappa_h$	r_0/a	am_π	am_ρ	am_K	am_D	$am_{\chi_l}^{PCAC}$
0.1690	2.222(54)	0.8237(13)	0.9684(20)	0.9231(11)	1.3192(87)	0.12113(40)
0.1695	2.503(41)	0.7329(11)	0.8916(15)	0.8652(11)	1.2827(58)	0.09738(34)
0.1700	2.812(48)	0.5857(18)	0.7631(35)	0.7739(12)	1.223(23)	0.06417(44)
0.1702	2.87(16)	0.5082(26)	0.7038(39)	0.7379(22)	1.187(21)	0.04837(30)
0.1704	3.28(12)	0.3695(22)	0.6041(44)	0.6553(21)	1.110(31)	0.02569(55)
0.1705	3.31(13)	0.3433(52)	0.5913(83)	0.6480(18)	1.080(35)	0.02117(53)
0.1706	4.50(20)	0.4331(74)	0.780(35)	0.6756(13)	0.943(46)	-0.0428(22)
0.1708	4.378(37)	0.4721(81)	0.843(15)	0.7004(18)	0.983(52)	-0.0492(31)
0.1710	4.59(16)	0.508(11)	0.812(16)	0.7216(17)	0.957(20)	-0.0569(26)

Figures

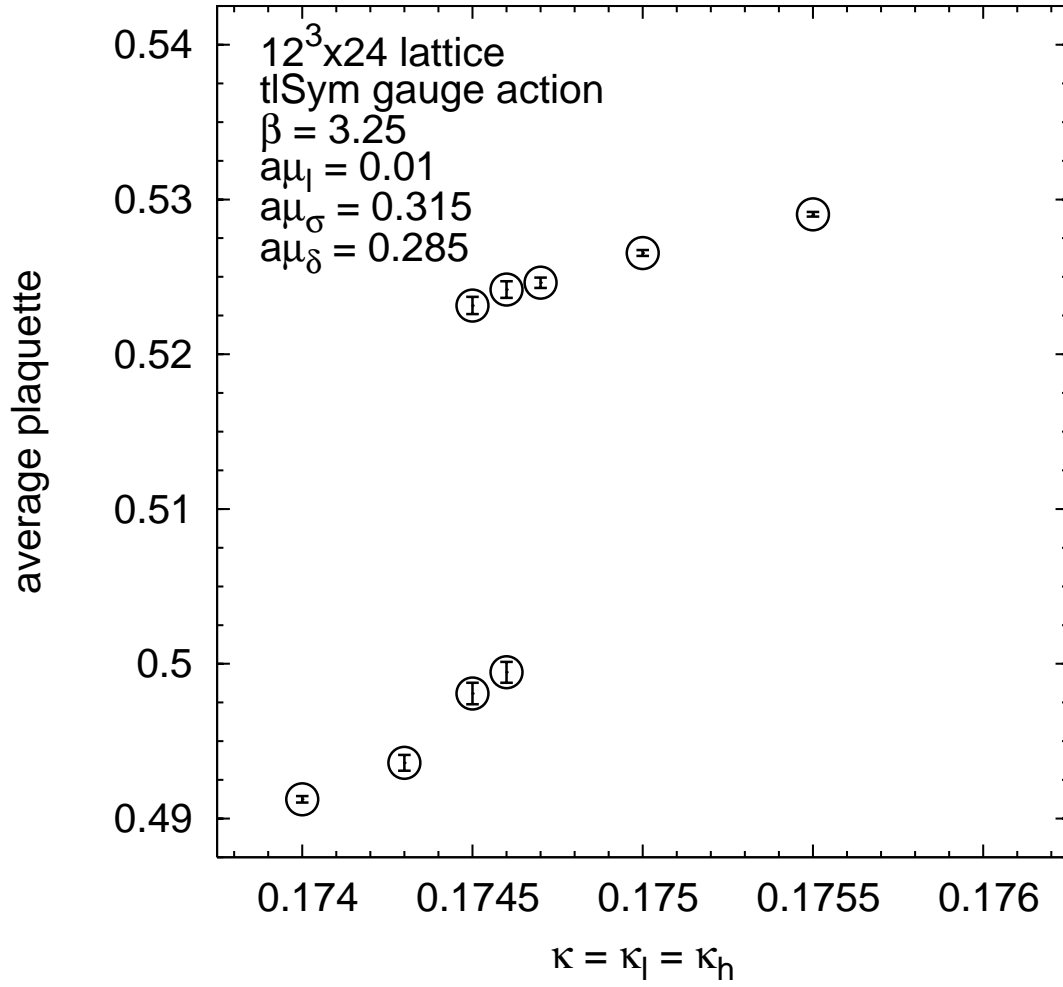


Figure 1: *The average plaquette on $12^3 \cdot 24$ lattice at $\beta = 3.25$, $a\mu_l = 0.01$, $a\mu_\sigma = 0.315$, $a\mu_\delta = 0.285$ as a function of $\kappa \equiv \kappa_l = \kappa_h$.*

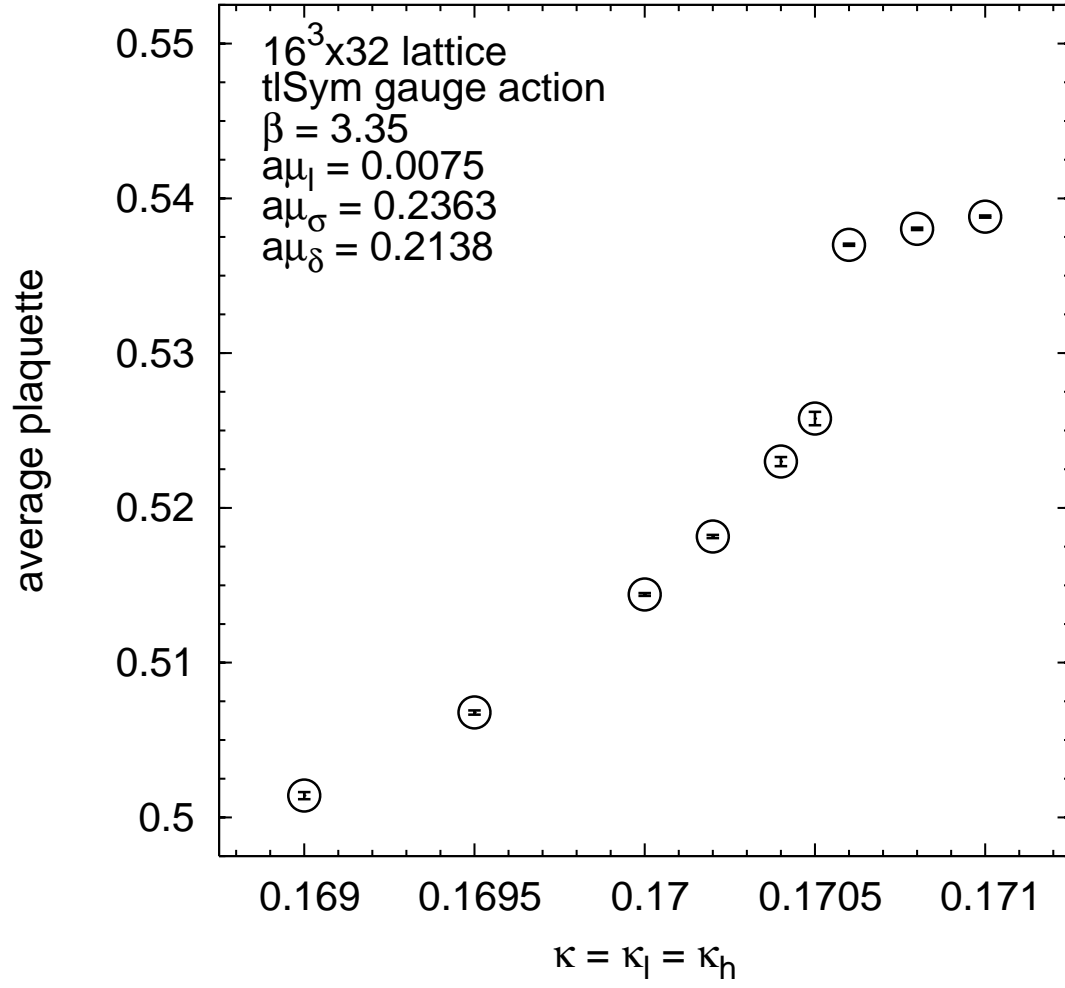


Figure 2: *The average plaquette on $16^3 \cdot 32$ lattice at $\beta = 3.35$, $a\mu_l = 0.0075$, $a\mu_\sigma = 0.2363$, $a\mu_\delta = 0.2138$ as a function of $\kappa \equiv \kappa_l = \kappa_h$.*

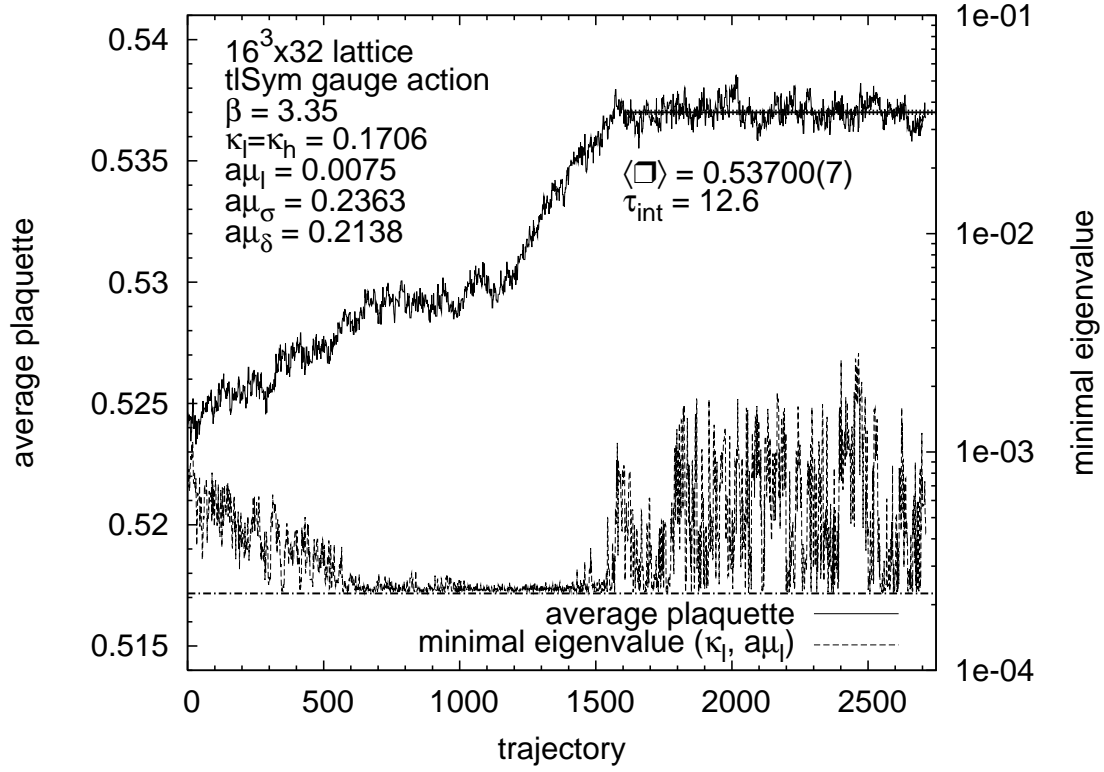


Figure 3: Run history on a $16^3 \cdot 32$ lattice at $\beta = 3.35$, $a\mu_l = 0.0075$, $a\mu_\sigma = 0.2363$, $a\mu_\delta = 0.2138$, $\kappa_l = \kappa_h = 0.1706$. This run started from a previous one at $\kappa = 0.1705$. On the horizontal axis the number of PHMC-trajectories (of length $\Delta\tau = 0.4$) is given. The average plaquette (upper curve, left scale) and the smallest eigenvalue of the squared preconditioned fermion matrix λ_{\min} (lower curve, right scale) are shown. The horizontal lines indicate the average plaquette after equilibration and the absolute minimum of λ_{\min} , respectively.

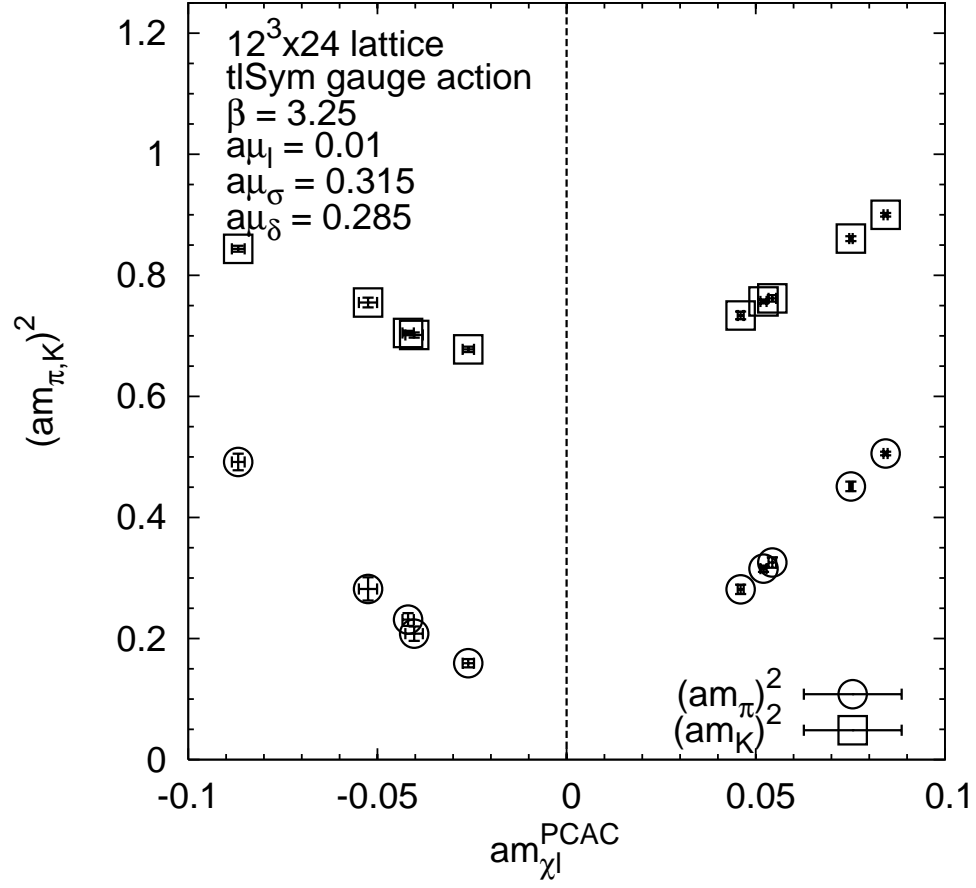


Figure 4: The mass-squared of pion and kaon as a function of the untwisted PCAC quark mass on a $12^3 \cdot 24$ lattice at $\beta = 3.25$, $a\mu_l = 0.01$, $a\mu_\sigma = 0.315$, $a\mu_\delta = 0.285$.

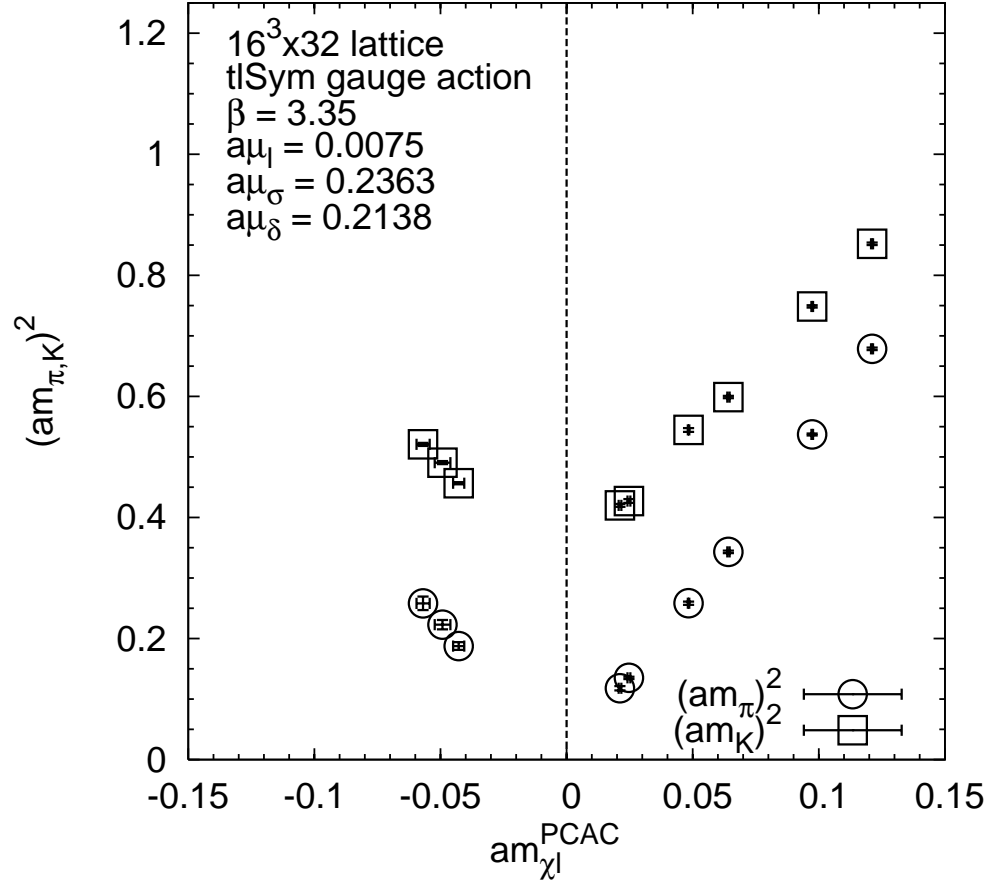


Figure 5: The mass-squared of pion and kaon as a function of the untwisted PCAC quark mass on a $16^3 \cdot 32$ lattice at $\beta = 3.35$, $a\mu_l = 0.0075$, $a\mu_\sigma = 0.2363$, $a\mu_\delta = 0.2138$.

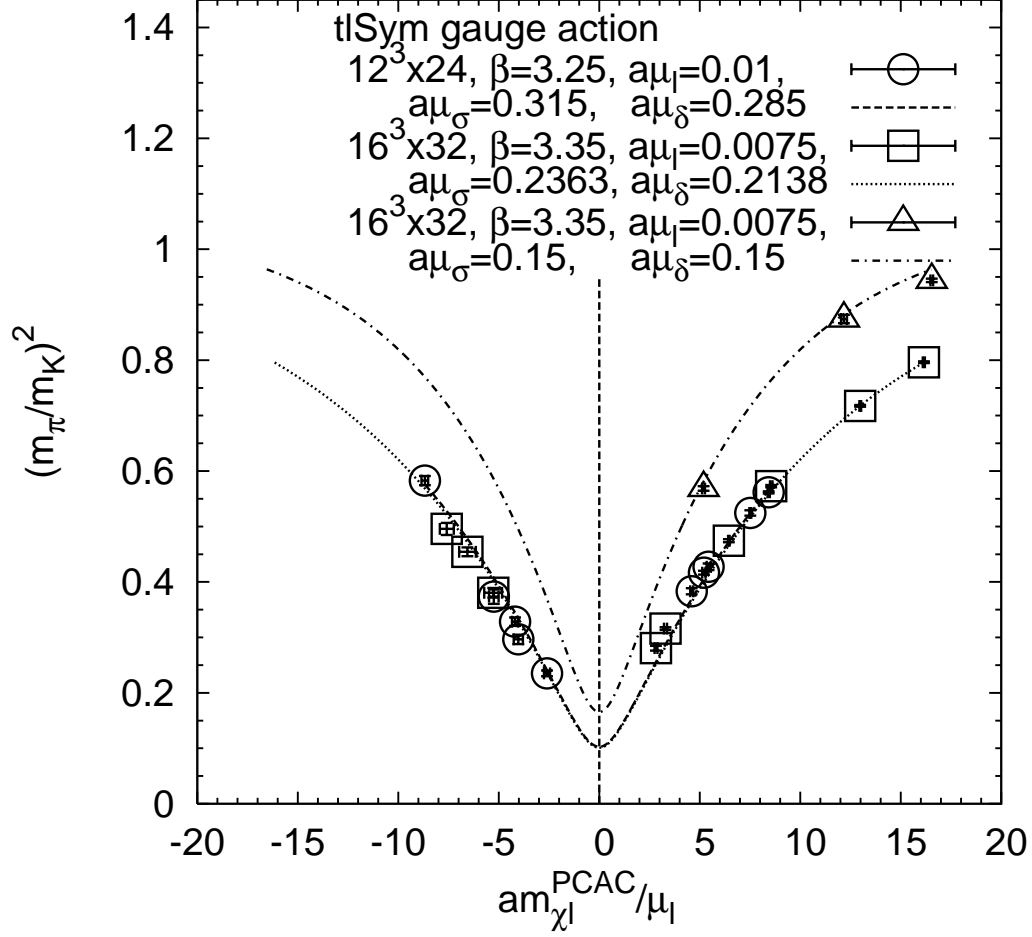


Figure 6: *Lowest order ChPT fit of the squared pion to kaon mass ratio as a function of the untwisted PCAC quark mass. Squares and triangles are data at $\beta = 3.35$, $\mu_l = 0.0075$ for $\mu_\sigma = 0.2363$, $\mu_\delta = 0.2138$ and $\mu_\sigma = 0.15$, $\mu_\delta = 0.15$, respectively. The fit to the formulas (57)-(58) gives $Z_P/Z_S = 0.446$. Circles are data at $\beta = 3.25$, $\mu_l = 0.01$, $\mu_\sigma = 0.315$, $\mu_\delta = 0.285$. The fit gives in this case $Z_P/Z_S = 0.457$.*